

Plastic Flow through Taper Dies: A Three-dimensional Analysis

Laxmi Narayan Patra, Susanta Kumar Sahoo, Mithun Kumar Murmu

Abstract—The plastic flow of metal in the extrusion process is an important factor in controlling the mechanical properties of the extruded products. It is, however, difficult to predict the metal flow in three dimensional extrusions of sections due to the involvement of re-entrant corners. The present study is to find an upper bound solution for the extrusion of triangular sectioned through taper dies from round sectioned billet. A discontinuous kinematically admissible velocity field (KAVF) is proposed. From the proposed KAVF, the upper bound solution on non-dimensional extrusion pressure is determined with respect to the chosen process parameters. The theoretical results are compared with experimental results to check the validity of the proposed velocity field. An extrusion setup is designed and fabricated for the said purpose, and all extrusions are carried out using circular billets. Experiments are carried out with commercially available lead at room temperature.

Keywords—Extrusion, Kinematically admissible velocity field Spatial Elementary Rigid Region (SERR), Upper Bound Analysis

I. INTRODUCTION

EXTRUSION, as a plastic flow of metal process, has definite advantages over rolling for the production of three-dimensional section shapes. Bars of polynomial sections, with or without re-entrant corners, can be formed from cylindrical available billets by extrusion through flat faced/ tapered/ curved dies with or without lubrication. For extrusion of sections, converging dies with lubrications is more preferred to flat dies or square dies, as it provides a gradual change in shape and reduction of the area simultaneously.

Despite the advantage of converging dies, a few theoretical approaches to the extrusion processes have been published. Nagpal and Altan [4] introduce the stream function to express three-dimensional flow in die and analyzed the force of extrusion from round billet to elliptical bars. Basily and Sansoml [1] made an upper bound analysis on drawing of square sections from round billets by using triangular element at entry and exit of the die. A method employing a discontinuous velocity field was proposed by Gatto and Giarda [2]. This method is based on discretizing the deformation zone into elementary rigid regions. In such a

scenario, the rigid regions have a constant internal velocity and the deformation is assumed to occur at the interfaces of these regions. The rigid element assumption limits the use of this technique to problems with flat boundaries. Further, Gatto and Giarda's formulation appears suitable for problems where billet and product sections are similar. Kar and Das [3] modified this technique to solve problems with dissimilar billet and product sections. However, their formulation was also limited to problems with flat boundaries and, as such as the analysis of extrusion from round billets is excluded from their formulation. However, Sahoo and Kar [5] used the reformulated spatial elementary rigid region (SERR) technique for the analysis of round-to-square extrusion. Sahoo, Kar and Singh [6] apply the reformulated SERR technique to extrusion of round-to-hexagon shapes through linearly converging dies. Sahoo [7] implement reformulated SERR technique to extrusion of T-section from round billet through straightly converging die. SERR technique and upper-bound analysis are analyzed for different sections through straight and linearly converging dies [8]-[10].

The present study is aimed to approximate the curved boundary by a series of planes and then applying the modified SERR technique to the series of resulting sub-zones of deformation for the extrusion of triangle section from round billets through converging dies. By using this method, normalized extrusion pressure has been calculated in terms of equivalent semi-cone angle, reduction of cross-sectional area and coefficient of friction between die surface and extruded material.

II. THEORETICAL ANALYSIS

A. The SERR Technique

In the SERR technique, the deformation zone is envisaged to consist of tetrahedral rigid blocks and each block separated from other by planes of velocity discontinuity. Each rigid block has its own internal velocity vector consistent with the bounding conditions. The components of these velocity vectors are determined by solving the set of velocity equations generated when the mass continuity condition is applied to the bounding faces of these basic blocks. Therefore, the basic blocks must be tetrahedral in shape for the velocity field so generated to be unique.

In case of metal deformation in a closed conduit, like extrusion, the deformation zone consists of subzones which may be tetrahedral, pyramidal or prismatic or a combination of these shapes. The pyramidal and prismatic subzones are

Laxmi Narayan Patra is with the National Institute of Technology Rourkela, Rourkela, Orissa, INDIA (phone: +91-9437204005; fax: 0661-2462999; e-mail: 508me607@gmail.com).

Susanta Kumar Sahoo is with the National Institute of Technology Rourkela. He is now with the Department of Mechanical Engineering National Institute of Technology Rourkela, Rourkela, Orissa, INDIA

M. K. Murmu is with the National Institute of Technology Rourkela. He is now with the Department of Mechanical Engineering National Institute of Technology Rourkela, Rourkela, Orissa, INDIA

ultimately to be subdivided into tetrahedral blocks. This subzone can be divided into two tetrahedrons thereby providing two schemes of discretizing a pyramid into tetrahedrons. Since each bounding face of a tetrahedron is triangular, equation of the plane containing a face can be determined from the coordinates of the vertices of the corresponding triangular face. Let the equation of the plane containing i^{th} face of the assembly of tetrahedrons in pyramid.

$$\phi_i(x, y, z) \equiv C_{1i}x + C_{2i}y + C_{3i}z + 1 = 0 \quad (1)$$

As stated above, the coefficients C_{1i} , C_{2i} and C_{3i} are known using the coefficients of the vertices. The unit normal vector associated with this face is then given by

$$\hat{n} = \frac{\nabla \phi}{|\nabla \phi|} \quad (2)$$

Then the mass continuity condition (or, sometimes called the volume constancy condition) dictates that

$$\hat{n} \cdot V_1 = \hat{n} \cdot V_2 \quad (3)$$

Here, the V_1 and V_2 are the velocities on both sides of the i^{th} face under consideration. Velocity equations such as (3) can be set up for all the faces in the assembly of tetrahedrons. The boundary conditions on velocity are also enforced through (3). For example, if a face lies on the dead metal surface (or the die wall in the case of tapered die) or a plane of symmetry, the appropriate side of (3) is set equal to zero to enforce the condition that no mass flow occurs normal to such faces. The simultaneous solution of the set of velocity equations yields the velocity field in its totality. The velocity of the product (direction known) is also obtained from the solution and serves as a check on the computational procedure since its magnitude can be independently determine from the prescribed billet velocity and the area ratio. These considerations also apply when the subzone is a single tetrahedron or a prism which can be divided into three tetrahedrons in six different ways.

B. Present Problem

In this study, plastic flow of metal through taper die, it is assumed that the centroid of the die aperture lies on the billet axis. This assumption is necessary so that the product remains straight as it comes out of the die orifice.

For the sake of the present analysis, it is assumed that the centroid of the die aperture lies on the billet axis. This assumption is necessary so that the product remains straight as it comes out of the die orifice.

As mentioned earlier, the SERR technique can be applied where there are plane boundaries. Hence, the curved surface is to be replaced by planar surfaces so as to accommodate the SERR analysis. For the present analysis the authors have

approximated the round billet by a 12-sided regular polygon (Fig. 2). This polygon was chosen since there is a negligible



Fig. 2 Variation of Exit velocity with no of sides of approximate polygon

change of final computed value by further increasing the number of sides. To approximate the circular cross-section of the billet into a regular polygon, the cross-sectional area of the billet and the area of the approximating polygon must be maintained equal. This condition is enforced through the relation

$$\pi R^2 = M \frac{1}{4} L^2 \cot\left(\frac{\theta}{2}\right) \quad (4)$$

From considerations of symmetry, only one half of the deformation zone (domain of interest) is considered for this analysis. The subzones of deformation can be delineated in the domain of interest by taking suitably located floating point (points whose locations are not a priori known). The resulting pyramid, prism and tetrahedrons are the ultimate deformation sub-zone for this SERR formulation. This single point formulation gives rise to two pyramids (12-5-6-11-10 and 12-8-7-9-11) and five tetrahedrons (11-12-10-2, 3-12-10-4, 4-12-10-5, 6-12-11-7 and 7-12-11-8). Hence, it results in nine tetrahedrons and the number of global schemes of discretization is 4. All these tetrahedral elements are interconnected and are separated from each other by common triangular faces (planes of velocity discontinuity). These basic SERR blocks in their totality have 28 triangular bounding faces. Applications of (3) to all these faces yield 28 velocity equations which in turn give an equal number of velocity components upon simultaneous solution. (discretization details summarized in Table 1) Similarly double point formulation can be done.

TABLE I
SUMMARY OF DISCRETIZATION SCHEMES

| Item | single point formulation |
|-------------------------------|---|
| Types of sub-zones | 2 pyramids and 5 tetrahedrons |
| No. of SERR blocks | $2 \times 2 + 5 \times 1 = 9$ |
| No. of discretization schemes | $2 \times 2 = 4$ |
| No. of triangular faces | 28 |
| No. of velocity component | $9 \times 3 = 27$ for 9 SERR + 1 at exit, Total=28 |

C. The Upper Bound Analysis

The upper bound theorem states that among all kinematically admissible velocity fields, the actual one minimizes the function J, where

$$J = J_1 + J_2 + J_3 \tag{5}$$

In which:

$$J_1 = \left(\frac{2\sigma_o}{\sqrt{3}} \right) \int_v \left[\frac{1}{2} \epsilon_{ij} \epsilon_{ij} \right]^{\frac{1}{2}} dv \tag{6}$$

= work required for internal deformation

$$J_2 = \left(\frac{\sigma_o}{\sqrt{3}} \right) \int_{A_i} |\Delta V_i| dA_i \tag{7}$$

= power dissipated at the surface Ai of velocity discontinuity

$$J_3 = \left(\frac{m\sigma_o}{\sqrt{3}} \right) \int_{A_{ij}} |\Delta V_i| dA_{ij} \tag{8}$$

= work required to overcome friction if the ith face is a die-work piece interface

In the present case, the velocity is constant inside a rigid block and, therefore, the strain rate components, ϵ_{ij} , are all zero thereby making J_1 equal to zero. Further, the die and work piece are not in contact because of the presence of the dead metal zone in between. Thus, J_3 is also zero. The velocities inside the rigid blocks being uniform, ΔV is uniform over the whole surface area of a velocity discontinuity surface. So J_2 becomes, for all the faces of velocity discontinuity,

$$J_2 = \left(\frac{\sigma_o}{\sqrt{3}} \right) \sum_{i=1}^{i=N} |\Delta V_i| A_i \tag{9}$$

Thus, ultimately we have

$$J = J_2 \tag{10}$$

The non-dimensional average extrusion pressure is then calculated as:

$$\frac{P_{av}}{\sigma_o} = \frac{J}{A_b V_b \sigma_o} \tag{11}$$

D. Computation

Using a suitable analytical model, computation is carried out.

It consists of following steps:

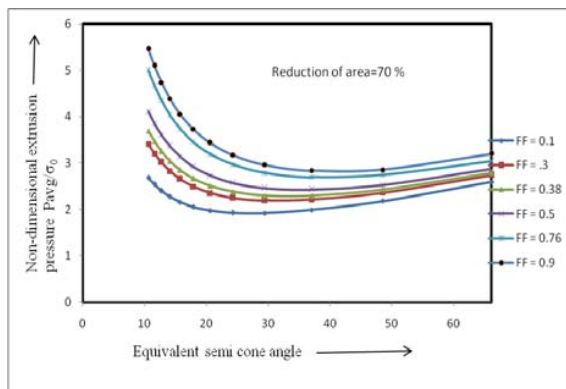
1. Determine the co-efficient of velocity equation of the planes containing bounding faces of tetrahedral block.

2. Determine the co-efficient of velocity equation by applying the mass continuity condition to respective planes.
3. Magnitude of velocity discontinuity is found out by algorithm. This solution also determines exit velocity, with serves as check on computation. Since exit velocity can be independently calculated using billet velocity and the area reduction.
4. Computing deformation work by (5) and non-dimensional extrusion pressure by (10).
5. Optimizing non-dimensional extrusion pressure with respect to variable parameter $X_{12}, Y_{12}, Z_{12}, X_{13}, Y_{13}, Z_{13}$, using multivariable unconstraint routine.

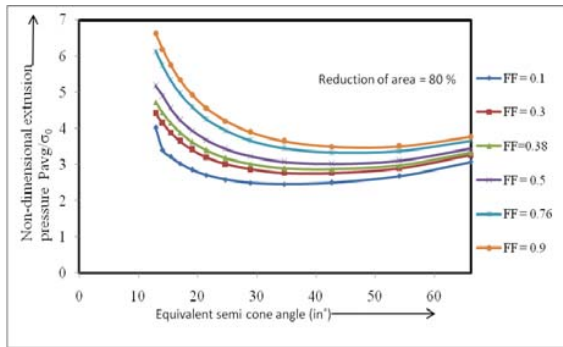
All the computation is carried out with a suitable subroutine of tetrahedron, pyramid, and prism imposed with different alternatives. Fig. 2 illustrate the variation of non-dimensional extrusion pressure with equivalent cone angle at area reduction 70%, 80% and 85% for different friction factor respectively. Fig. 3 shows the variation of non-dimensional extrusion pressure with percentage of area reduction at equivalent semi-cone angle 20° for different friction factor.

E. The optimization parameters

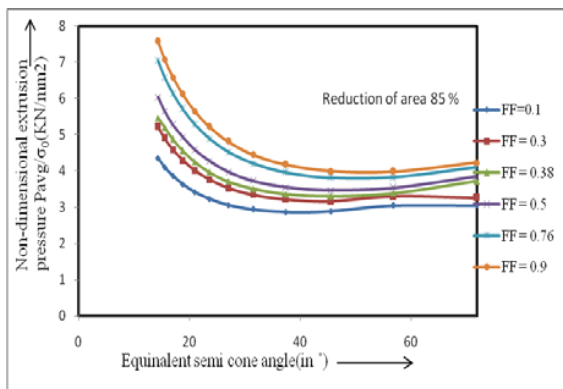
For the single point formulation, the floating point lies on the plane of symmetry. Thus, in total there are two undetermined co-ordinates, which serve as optimization parameters to minimize the extrusion pressure for this formulation. Here, it is to be noted that the die length is represented by the equivalent semi-cone angle. The equivalent semi-cone angle is defined as the semi-cone angle of a conical die where the reduction area is the same as that of polygonal sections. For a double point formulation one of the floating points lays on plane of symmetry having two undetermined co-ordinates. Second floating point lies anywhere inside deformation zone having three undetermined co-ordinates. Height of deformation zone is an additional optimizing parameter.



(a) 70% area reduction



(b) 80% area reduction



(c) 85% area reduction.

Fig. 2 Variation of non-dimensional extrusion pressure with equivalent semi cone angle for different area reduction

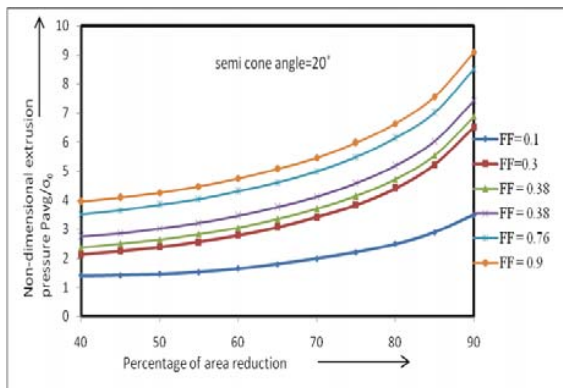


Fig. 3 Variation of non-dimensional extrusion pressure with percentage of area reduction

III. EXPERIMENTAL ANALYSIS

A. Apparatus

The apparatus (fig.4) primarily, consists of five parts; namely, the container having a cylindrical hole, the die holder, the base plate, the extruding punch, and the supporting plate. The dies used in the present series of experiments are made of two split

halves for easy removal of the extruded product. The dies are so made that the respective centers of gravity of both shapes lay on the billet axis. Experiments are conducted for different reductions (72.78%, 80.78% and 87.41%) and both lubrication and dry conditions.

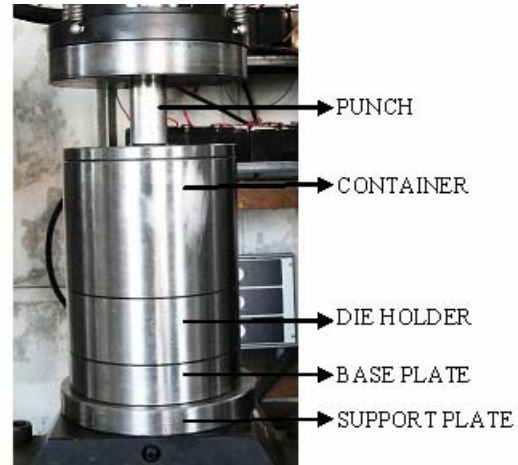


Fig 4 Experimental setup

B. Billet Specimen

Cylindrical billet specimens of commercially available lead are taken as work material for the above purpose. The specimens are prepared from commercially available ingot. From the ingot required shape specimens were first casted using open type green sand casting method. The casted lead is turned in a lathe to required diameter and parted to required length. All specimens before use are annealed in boiling water for a period of two hours.

C. Experimentation

The die-sets, the die holder and the inside faces of the extrusion chamber were cleaned with carbon tetrachloride before starting the tests. The two halves of the die set were then pushed fitted into the die holder and the total assembly is perfectly assembled by screwing four bolts. Before assembling the inner surfaces of the container and dies are lubricated with grease. Specimen is also lubricated and placed inside the container. One face of the specimen is chamfered for easy insertion into the dies. The full assembly is then placed on the lower table of the Instron (UTM). The friction factor is found to be 0.38 for the lubrication (from ring compression test) and 0.76 for dry condition. Cylinders with a 32 mm \times 48 mm ($H/D = 1.5$) are used to obtain the stress-strain curve by a compression test at room temperature. The compression rate is maintained same as that adapted for the experiments. The average flow stress of the used material is found to be 0.250 kN/mm². The speed of UTM is maintained uniform approximately at 1.5mm per minute to minimize rate effect. Load versus stroke is plotted and the nature of variation

is observed. Experiments were conducted for all reductions; Fig.5 shows the extruded product with lubrication condition.



Fig. 5 Photograph of final products at different reductions

IV. RESULT AND DISCUSSION

The variation of compressive load with extension was determined from the extrusion test. From fig.5 and fig. 6 it has been seen that a typical diagram consists of two stages; namely

1. A coining stage in which load increases gradually and reaches peak value due to initial compression of billet.
2. A steady stage of extrusion in which load maintains approximately a constant value up to the end of the extrusion.

The average load corresponding to the second stage consider as the extrusion load. The value of uniaxial yield stress in compression σ_0 , is calculated from stress strain characteristics plot of lead and non- dimensional mean extrusion pressure (P_{avg}/σ_0) is calculated.

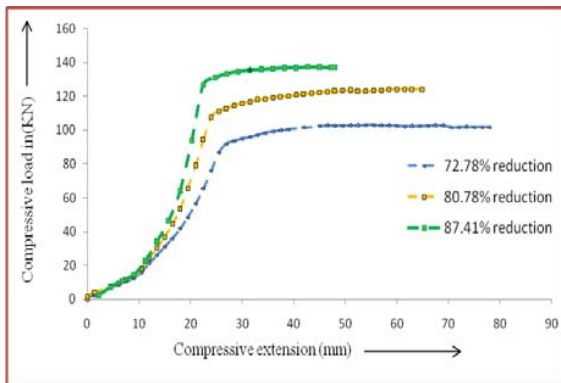


Fig.6 Variation Punch load vs. punch travel for lubricated condition

Referring to Figure 6, the extrusion load decreases marginally with punch displacement for lubricated condition during steady state stage, but it is more prominent for dry condition. This may be attributed to the high friction exist between billet and container in dry condition, which decreases with the length of the billet.

The comparison of experimental values with that of theoretical results shows the difference remains within 10 percent.

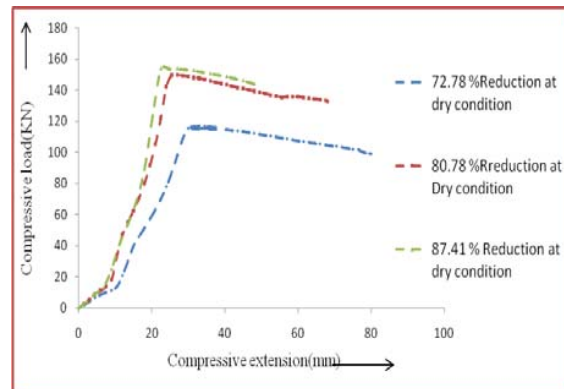


Fig.6 Variation Punch load vs. punch travel for dry condition

TABLE II
COMPARISON OF EXPERIMENTAL AND COMPUTED RESULTS

| Reduction % | Friction Factor | Equivalent Semi cone angle | P_{avg}/σ_0 (Computed) | P_{avg}/σ_0 (Experimental) | Difference % |
|-------------|-----------------|----------------------------|-------------------------------|-----------------------------------|--------------|
| 72.78 | 0.76(Dry) | 10.56 | 5.72 | 5.69 | 0.52 |
| 80.78 | 0.76(Dry) | 12.33 | 6.51 | 6.80 | -4.45 |
| 87.41 | 0.76(Dry) | 14.09 | 7.65 | 7.63 | 0.26 |
| 72.78 | 0.38(Wet) | 10.56 | 4.69 | 4.99 | -6.39 |
| 80.78 | 0.38(Wet) | 12.33 | 5.38 | 5.36 | 0.37 |
| 87.41 | 0.38(Wet) | 14.09 | 6.45 | 6.42 | 0.46 |

V.CONCLUSION

From the present investigation following conclusions may be drawn:

1. The upper bound analysis of extrusion of different sections taper dies can carry out by using discontinuous velocity field (modified SERR technique). These techniques provided a better method of analysis for this type of section extrusion, which are difficult by the continuous velocity field formulation.
2. Increasing the percentage of reduction accompanying with increase in extrusion loads.
3. Using this solution, the optimal die geometry (equivalent semi-cone angle) can be obtained for different area reductions and friction conditions.
4. Comparison made with existing theoretical and experimental results shows that the present solution can predict reasonable upper-bound extrusion pressure.

5. The present method can be extended to obtain the solution of generalized problems of non-axisymmetric extrusion or drawing through taper dies.

REFERENCES

- [1] Basily, B.B. & Sansome, D.H. 1976, "Some theoretical considerations for the direct drawing of section rod from round bar", *International Journal of Mechanical Sciences*, vol. 18, no. 4, pp. 201-208.
- [2] Gatto, F. & Giarda, A. 1981, "The characteristics of the three-dimensional analysis of plastic deformation according to the SERR method", *International Journal of Mechanical Sciences*, vol. 23, no. 3, pp. 129-148.
- [3] Kar, P.K. & Das, N.S. 1997, "Upper bound analysis of extrusion of I-section bars from square/rectangular billets through square dies", *International Journal of Mechanical Sciences*, vol. 39, no. 8, pp. 925-934.
- [4] Nagpal, V. & Altan, T. 1975, "Analysis Of The Three-Dimensional Metal Flow In Extrusion Of Shapes With The Use Of Dual Stream Functions.", *Proc. Third N.Am. Met. Res. Conf., Pittsburgh, Pennsylvania*, pp 26-40.
- [5] Sahoo, S K and kar, P K, 2000, Round-to-Square Extrusion Through Taper Die: A Three-dimensional Analysis. *Manufacturing Technology Proc. of 19th AIMDT Conf.*
- [6] Sahoo, S.K., Kar, P.K. & Singh, K.C. 1999, "Numerical application of the upper-bound technique for round-to-hexagon extrusion through linearly converging dies", *Journal of Materials Processing Technology*, vol. 91, no. 1, pp. 105-110.
- [7] Sahoo, S.K. 2003, "An analysis of plastic flow through polygonal linearly converging dies: As applied to forward metal extrusion", *Journal of Materials Processing Technology*, vol. 132, no. 1-3, pp. 286-292.
- [8] Sahoo, R.K., Kar, P.K. & Sahoo, S.K. 2003, "3D upper-bound modeling for round-to-triangle section extrusion using the SERR technique", *Journal of Materials Processing Technology*, vol. 138, no. 1-3, pp. 499-504.
- [9] Sahoo, R.K., Samantaray, P.R., Sahoo, S.K., Sahoo, B. & Kar, P.K. 2009, "Round-to-channel section extrusion through linearly converging die: A three-dimensional analysis", *International Journal of Advanced Manufacturing Technology*, vol. 41, no. 7-8, pp. 677-683.
- [10] Sahoo, S.K., Sahoo, B., Patra, L.N., Paltasingh, U.C. & Samantaray, P.R. 2010, "Three-dimensional analysis of round-to-angle section extrusion through straight converging die", *International Journal of Advanced Manufacturing Technology*, vol. 49, no. 5-8, pp. 505-512.